Comparison of extension and compression triaxial tests for dense sand and sandstone

Alain Corfdir, Jean Sulem

Editorial Manager(tm) for Acta Geotechnica
Manuscript Draft

Manuscript Number: AGEO-D-07-00024R2

Title: Comparison of extension and compression triaxial tests for dense sand and sandstone

Article Type: Short Communication

Keywords: Compresssion test
Extension test
Friction angle
Sand
Sandstone

Corresponding Author: Dr Alain CORFDIR,

Corresponding Author's Institution: ENPC

First Author: Alain CORFDIR

Order of Authors: Alain CORFDIR; Jean SULEM, Ph .D

Abstract: It is generally observed that for a given confining pressure the friction angle at peak strength of dense sand deduced from triaxial compression test is smaller than the one obtained from extension tests. In fact, this conclusion depends essentially on the way to take into account the global confinement condition. In this paper, we show that when there is no significant grain crushing, the dependence of the maximum friction angle with the average of minor and major principal effective stress is similar for compression and extension tests. A similar result is obtained for sandstones when the failure mode involves a shear failure plane.

authors' response to reviewers' comments

Click here to download authors' response to reviewers' comments: answer5.doc

After sending the first revised version, we noticed that reviewer # 3 had given an annoted version of our initial manuscript on the web site. So, this final revision takes his annotations into account. We apologize for this mistake.

The figures have been redrawn according to your remarks.

Comparison of extension and compression triaxial tests for dense sand and sandstone

A. CORFDIR[1]

J. SULEM

Université Paris-Est, UR Navier, CERMES, Ecole Nationale des Ponts et Chaussées, 6 et 8 avenue Blaise Pascal, 77455 Marne-la-Vallée, France

Abstract

It is generally observed that for a given confining pressure the friction angle at peak strength of dense sand deduced from triaxial compression test is smaller than the one obtained from extension tests. In fact, this conclusion depends essentially on the way one takes into account the global confinement condition. In this paper, we show that when there is no significant grain crushing, the dependence of the maximum friction angle with the average of minor and major principal effective stress is similar for compression and extension tests. A similar result is obtained for sandstones when the failure mode involves a shear failure plane.

Key words: Compression test, extension test, friction angle, sand, sandstone

Submitted to Acta Geotechnica,
Revised version, April 2008

[1] Corresponding author, Corfdir@cermes.enpc.fr

1 Introduction

Comparison of results from extension and compression tests on sands is an old dispute: is the friction angle at peak higher in extension or in compression ? This question is a particular point in the wider debate on the relationship between the friction angle and the Lode angle or the factor $b=(\sigma_2-\sigma_3)/(\sigma_1-\sigma_3)$ (Lade, 2006). Tests results collected by Wu and Kolymbas (1991) showed that for loose sand no general conclusion can be drawn and that for dense sand the friction angle is higher for extension tests than for compression tests performed at the same confining pressure. Special attention must be paid to the difficulties met when carrying out extension tests, the more specific one being the necking phenomenon which makes extension test unstable (Lade, 2006, Yamamuro and Lade, 1995, Wu and Kolymbas, 1991). Wu and Kolymbas (1991) listed the possible artefacts of extension tests such as the influence of the membrane, the effect of the weight of the sample, the effect of non-homogenous deformation. This last effect was corrected by measuring the local lateral deformation with a special device (Kolymbas and Wu, 1989) and evaluating the axial stress with a corrected area. Yamamuro and Lade (1995, 1996) avoided necking of the sample by using membranes reinforced by metal plates as described in (Lade et al., 1996). In this paper, the method of comparison of the measured friction angles is critically discussed in order to better understand the different values measured in the case of dense sands in dry or drained condition. High pressure tests where grain crushing can cause a change of behaviour (Yamamuro and Lade, 1996) are not considered in this study. The difference in measured friction angle appears to be due to the influence of stress level. Finally, the comparison is extended to cohesive granular media such as sandstones. For tests without brittle tension failure, the tangent friction angle is compared for compression and extension tests. We emphasize the fact that the comparison is made for the maximum mobilized friction angle so that only the failure state is discussed and not the complete constitutive behaviour of the material. This failure state may be the result of strain localisation. In particular, we are interested in discussing the appropriate stress quantity which controls the stress-dependent character of the friction angle at failure.

2 Comparison of experimental results for dense sand

Only a limited number of tests data allowing the comparison of extension and compression results are available in the literature. As stated above, extension tests are especially difficult to perform and we use here two data sets, one from (Kolymbas and Wu, 1990, Wu and Kolymbas, 1991), and the other one from (Yamamuro and Lade, 1996).

For both data sets, the samples were built using a pluviation technique. Wu and Kolymbas (1991) tested a dry Karlsruhe medium sand with D_{50}=0.395 mm and average relative density 100%. We also refer to the compression tests of Kolymbas and Wu (1990) on the same material. Yamamuro and Lade (1996) tested a water saturated Cambria sand in drained conditions. This sand is uniformly graded with a grain size of 0.83 to 2 mm and an average relative density 89.5 %. Among the test data of Yamamuro and Lade, we selected those for which no important grain crushing was observed. This condition gives a limit of about 8 MPa for the shear stress $|\sigma'_a - \sigma'_r|$ where σ'_a is the (effective) axial stress and σ'_r is the confining stress. In the following we will consider total stresses for dry samples and effective stresses for saturated samples tested in drained conditions. For simplicity, the total stress (for dry samples) and the effective stress (for saturated samples) are both denoted by σ.

For cohesionless materials, the friction angle for each test has been simply evaluated in the Mohr plane as the secant angle at maximum shear stress $\sin\phi = |\sigma_a - \sigma_r|/(\sigma_a + \sigma_r)$. This definition does not imply a priori the validity of Mohr-Coulomb criterion, nor the independence from the intermediate principal value of the stress tensor.

The results of Wu and Kolymbas (1990, 1991) are presented in Figs. 1, and 2 where the maximum friction angle in compression and in extension is plotted vs. the confining stress σ_r and vs. the mean stress $p = (2\sigma_r+\sigma_a)/3$ at peak. As shown by these plots, the difference between the friction angle in compression and in

extension plotted against the confining pressure σ_r is reduced when the friction angle is plotted against the mean stress.

Figure 1

Figure 2

The difference is reduced even more by plotting the measured values of friction angle as a function of $s = (\sigma_a+\sigma_r)/2$ (Fig. 3). The same remarks can be made for the test results by Yamamuro and Lade (Figs. 4-5) for a large range of pressures.

Figure 3

Figure 4

Figure 5

3 Comparison of experimental results on sandstone

The same approach is now applied to sandstone which can be viewed as a cohesive granular material. Two sets of tests results have been published by Bésuelle (1999) and Bésuelle et al. (2000) for Woustwiller sandstone on one hand and by Sulem et al. (1999) and by Papamichos et al. (2000) on Red Wildmoor sandstone on the other hand. Their data are analysed in the following.

As it can be seen on Fig. 6 for Woustwiller sandstone, it is not possible to define a secant friction angle or a tangent friction angle for extension tests at relatively low confining pressure as for σ_r=10, 20 and 30 MPa, tensile failure occurs on a quasi-horizontal plane (Bésuelle et al., 2000). Thus, only the tests at higher confining pressure where shear failure occurs are considered hereafter. It is also observed on Fig. 6 that a unique envelope surface cannot be drawn for the Mohr circles of compression and extension tests with failure in the compressive regime. Consequently, the discussion herein will refer to the tangent friction angle.

Figure 6

The tangent friction angle is evaluated by considering the tangent line to two adjacent Mohr circles. This quantity is plotted as function of the X-coordinate of the middle point of the centre of the two circles (Figs. 7-8). The plots of Figs. 7, and 8 show that the friction angles in compression and extension lay on a unique curve when plotted as a function of $(\sigma_a+\sigma_r)/2$ (centre of the Mohr circle).

Figure 7

Figure 8

4 Discussion

4.1 Axisymmetric triaxial tests on loose sand or on dense sand at high confining pressure

The above results do not apply to loose sands. This has been checked for the tests of Wu and Kolymbas (1990) and of Lade and Bopp (2005). Fig. 9 shows the secant friction angle plotted versus $(\sigma_a+\sigma_r)/2$ for tests by Lade and Bopp (2005) on Cambria sand with an initial relative density of 30%. Even at low confining pressure, extension tests and compression tests do not lie on a single curve. The gap between the two curves is even larger when the friction angle is plotted versus the radial stress σ_r or the mean stress p.

On Fig. 9, a clear change is observed for the slope of the curve at high confining pressure (>10MPa) for the compression tests. In this range of confining pressure the friction angle is larger in compression than in extension. The same phenomenon is also observed for dense sands at high confining pressure (Yamamuro and Lade, 2006). The change of response at high confining pressure can be attributed to particles breakage which is different in compression and in extension. (Yamamuro and Lade, 2006).

For these two cases, a simple stress quantity cannot be found for describing the stress dependency of the friction angle in compression and in extension.

Figure 9

4.2 True triaxial tests on rocks and on sand

For different type of rocks tested in true triaxial conditions, Haimson (2006) has studied the effect of the intermediate principal stress on the maximal octahedral shear stress. He has shown that the octahedral shear stress at failure is a unique function of the mid-sum of the two extreme principal stresses. This does not imply that the failure criterion is independent of the intermediate stress as this quantity is accounted for in the expression of the octahedral shear stress. In particular for both compression and extension conditions the octahedral shear stress is $|\sigma_a - \sigma_r|$. Haimson's observation corroborates our finding that $\sin\phi = \frac{|\sigma_a - \sigma_r|}{\sigma_a + \sigma_r}$ is a unique function of $(\sigma_a + \sigma_r)/2$. For true triaxial tests on Santa Monica Beach sand (Wang and Lade, 2001), it has been observed that shear banding appears in hardening regime for 0.15<b<0.85, with $b = (\sigma_2 - \sigma_3)/(\sigma_1 - \sigma_3)$. In a quite similar way as for rocks, the octahedral shear stress seems to be better correlated with $(\sigma_1 + \sigma_3)/2$ than with $(\sigma_1 + \sigma_2 + \sigma_3)/3$ (Fig 10).

Figure 10

4.3 Choice of $(\sigma_a+\sigma_r)/2$ for describing stress-dependent friction

In triaxial condition, the study of the Mohr circles reduces to the study of the circle in any plane containing the axial direction. If the failure envelope can be drawn, for each value of secant angle there is a unique Mohr circle, the centre of which has its X coordinate equal to $(\sigma_a+\sigma_r)/2$ for both extension and compression loading cases. The failure envelope is very simply described by the secant friction angle as a function of $(\sigma_a+\sigma_r)/2$. It is the only natural choice which makes it

possible to check immediately whether the failure criterion is the same in compression and extension.

Stress dependency of the friction angle is commonly expressed in terms of the mean stress. This invariant is chosen by Yamamuro and Lade (1996) for comparing compression and extension tests. For isotropic materials, a functional basis of independent invariants consists of 3 elements. The usual basis is $p = \frac{1}{3}\sigma_{kk}$, $J_{2s} = \frac{1}{2}s_{ij}s_{ji}$ where $s_{ij} = \sigma_{ij} - p\delta_{ij}$ is the deviatoric stress tensor and $J_{3s} = \frac{1}{3}s_{ij}s_{jk}s_{kj}$. The mean stress p is the only linear stress invariant for isotropic systems. For axisymmetric triaxial tests, it can be easily proved that $(\sigma_a + \sigma_r)/2$ can be written in terms of stress invariants:

$$\frac{\sigma_a + \sigma_r}{2} = p + \frac{3}{4}\frac{J_{3s}}{J_{2s}} \qquad (1)$$

Thus the choice of $(\sigma_a+\sigma_r)/2$ is natural and is not in contradiction with invariant tensor theory.

4.4 Comparison of tests data and predicted values in the case of sands

All values of sin(φ) (extension and compression, Wu and Kolymbas and Yamamuro's tests) can be globally fitted as a power law of $s = (\sigma_a + \sigma_r)/2$. The best fit was found to be:

$$\sin\varphi = 0.62 * s^{-0.0645} \text{ (with } s \text{ in MPa)} \qquad (2)$$

Equation (2) can be rewritten as

$$|\sigma_a - \sigma_r| = 1.24\left(\frac{\sigma_a + \sigma_r}{2}\right)^{0.9355} \quad \text{(with } \sigma_a, \sigma_r \text{ in MPa)} \qquad (3)$$

The axial stress can be expressed as:

$$\sigma_a = s(1 + \sin\varphi(s)) \text{ (compression); } \sigma_a = s(1 - \sin\varphi(s)) \text{ (extension)} \qquad (4)$$

Using equation (3), we get:

$$\sigma_a = \sigma_r + 1.24\left(\frac{\sigma_a + \sigma_r}{2}\right)^{0.9355} \quad \text{(with } \sigma_a, \sigma_r \text{ in MPa) (compression);} \qquad (5a)$$

$$\sigma_a = \sigma_r - 1.24\left(\frac{\sigma_a + \sigma_r}{2}\right)^{0.9355} \quad \text{(with } \sigma_a, \sigma_r \text{ in MPa) (extension)} \qquad (5b)$$

The predicted values of σ_a versus σ_r given by (5) are compared with tests results in Fig. 11.

Figure 11

Predicted values and experimental data appear to be in good accordance on a large range of confining pressure for both extension and compression tests, even for data corresponding to the two different sands (Karlsruhe sand and Cambria sand).

4.5 Failure mechanism and tests results

Different failure mechanisms induce different maximal shear values for triaxial tests (e.g. Suzuki and Yamada, 2006) and for true triaxial tests (Lade, 2006). In the above related tests different failure modes (with no shear band, with an incomplete partially developed shear band, with a fully developed single shear band or with a system of several shear bands) have been obtained.

The tests data used for sand were not focussed on tracking shear band formation and evaluating its inclination. But Wu and Kolymbas (1991) mentioned shear

banding in extension tests for dense sand. It is well known that dense sand triaxial tests involve shear banding (Vardoulakis and Sulem, 1995). Concerning tests on Woustwiller sandstone, for the tests that have been compared (i.e. compression and extension tests with similar value of $(\sigma_a+\sigma_r)/2$), it has been found that the failure pattern is a unique failure plane in both cases. For Wildmore sandstone, all triaxial tests presented here have a shear band failure pattern (Papamichos et al., 2000).

Thus for the tests considered in this paper, when the appropriate data are available, the failure mode is similar for compression and extension when the secant friction angles (for sand) or tangent friction angles (for sandstone) are identical in compression and extension.

In the pre-localisation regime, triaxial tests conditions impose fixed principal stress directions whereas strain localisation allows for principal stress rotations. This phenomenon can be used for calibration out of plane shear moduli (Vardoulakis, 1980, Sulem et al. 1999, Desrues and Chambon, 2002). However an out of plane stress increment does not affect much the principal stresses. If we assume, as it is done here, that the failure criterion is isotropic then stress rotation induced by the strain localisation process does not affect the relation between the axial stress and the radial stress at failure. On the other hand, strain localisation can result in a stress-induced anisotropy of the material inside the shear band and could thus lead to an anisotropic failure criterion. A recent paper of Gajo et al. (2007) shows that although stress induced anisotropy affects the conditions for onset of strain localisation, the global response of sample is not much affected. Therefore, it is expected that stress induced anisotropy will not affect much the axial stress at failure.

5 Conclusion

The comparison of compression and extension triaxial tests on dense dry sands shows that when special care has been taken to prevent or to correct the effects of necking, the secant friction angle at failure is a unique function of $(\sigma_a+\sigma_r)/2$ for both loading cases. The comparison of compression and extension triaxial tests on sandstones shows also that the friction tangent angle is very similar in both cases (for the same value of $(\sigma_a+\sigma_r)/2$), when failure occurs with shear banding. When strain localisation occurs, a transition between the imposed axisymmetric strain mode and a plane strain mode takes place and thus our results suggest that whether the failure plane is formed in extension or in compression does not affect the stress-dependency of the maximum mobilized friction angle. Therefore, constitutive models which incorporate stress-dependency of the friction angle should be compatible with this result. This result does not hold for loose sands or for sands at high pressures. In the case of loose sands, this can be explained by the fact that the failure mechanism is different from the one of dense sands as no peak is observed in the stress-strain curve and no failure plane is formed. For the case of sands tested at high pressures, one could relate the different response to the different mechanism of particle breakage in compression and in extension.

Ackowledgements

The authors wish to thank Prof. Dimitrios Kolymbas for fruitful discussions.

References

BÉSUELLE P (1999) Déformation et rupture dans les roches tendres et les sols indurés : comportement homogène et localisation, thèse de l'Université Joseph Fourier – Grenoble.

BÉSUELLE P, DESRUES J, RAYNAUD S (2000) Experimental characterisation of the localisation phenomenon inside a Vosges sandstone in a triaxial cell. International Journal of Rock Mechanics & Mining Sciences 37: 1223-1237.

DESRUES J, CHAMBON R. (2002) Shear band analysis and shear moduli calibration. Int. J. Sol. Struct. 39, 3757-3776.

GAJO A., MUIR WOOD D., BIGONI D. (2007) On certain critical material and testing characteristics affecting shear band development in sand, Géotechnique, 57: 5, 449-461.

HAIMSON B (2006) True Triaxial Stresses and the Brittle Fracture of Rock, Pure applied Geophys, 163: 1101-1130.

KOLYMBAS D, WU W (1989) A Device for Lateral Strain Measurement in Triaxial Tests with Unsaturated Specimens. Geotechnical Testing Journal 12: 227-229.

KOLYMBAS D, WU W (1990) Recent results of Triaxial Tests with Granular Materials. Powder Technology 60: 99-119.

LADE PV, BOPP PA (2005) Relative density effects on drained sand behavior at high pressures. Soils and foundations 45: 1-13.

LADE PV, YAMAMURO JA, SKYERS BD (1996) Effects of shear band formation in triaxial extension tests. Geotechnical Testing Journal 19: 398-410.

LADE PV (2006) Assessment of test data for selection of 3-D failure criterion for sand. Int J Num Anal Meth Geomech 30: 307-333.

PAPAMICHOS E, TRONVOLL J, VARDOULAKIS I, LABUZ JF, SKJÆRSTEIN A, UNANDER TE, SULEM J (2000) Constitutive testing of Red Wildmoor sandstone. Mech Cohes-Frict Mater 5:1-40.

SULEM J, VARDOULAKIS I, PAPAMICHOS E, OULAHNA A, TRONVOLL J. (1999) Elasto-plastic modelling of Red Wildmoor sandstone. Mechanics of cohesive-frictional materials 4: 215-245.

SUZUKI K, YAMADA T (2006) Double Strain Softening and Diagonally Crossing Shear Bands of Sand In Drained Triaxial Tests. International Journal of Geomechanics 6: 440-446.

VARDOULAKIS I, (1980) Shear band inclination and shear modulus of sand in biaxial test. Int. J. Num. Anal. Meth. Geomech. 4, 103-119.

VARDOULAKIS I, SULEM J (1995) Bifurcation Analysis in Geomechanics, Chapman & Hall.

WANG Q, LADE PV (2001), Shear Banding in True Triaxial Tests and Its Effect on Failure on Sand. Journal of Engineering Mechanics 127: 754-761.

WU W, KOLYMBAS D (1991) On some issues in triaxial extension tests. Geotechnical Testing Journal 14: 276-287.

YAMAMURO JA, LADE PV (1995) Strain localization in extension tests on granular materials. Journal of Engineering Mechanics 121: 828-836.

YAMAMURO JA, LADE PV (1996) Drained Sand Behavior in Axisymmetric Tests at High Pressure. Journal of Geotechnical Engineering 122: 109-119.

Fig. 1 Secant friction angle as a function of radial stress; data from Wu and Kolymbas (1991), Kolymbas and Wu (1990)

Fig. 2 Secant friction angle as a function of mean stress p; data from Wu and Kolymbas (1991) Kolymbas and Wu (1990)

Fig 3 Secant friction angle versus $(\sigma_a+\sigma_r)/2$; data from Wu and Kolymbas (1991) Kolymbas and Wu (1990)

Fig. 4 Secant friction angle as a function of mean stress p'; data from Yamamuro and Lade (1996)

Fig. 5 Secant friction angle versus $(\sigma'_a+\sigma'_r)/2$; data from Yamamuro and Lade (1996)

Fig. 6 Mohr circles for Woustviller sandstones; solid lines: extension tests; dashed lines: compression tests (data from Bésuelle, 1999)

Fig. 7 Tangent friction angle versus $(\sigma_a+\sigma_r)/2$; Woustwiller sandstone; data from Bésuelle et al. (2000)

Fig. 8 Tangent friction angle versus $(\sigma_a+\sigma_r)/2$; Red Wildmoor sandstone; data from Papamichos et al. (2000)

Fig. 9 Secant friction angle versus $(\sigma'_a+\sigma'_r)/2$ for loose Cambria sand; data from Lade and Bopp, (2005)

Fig 10 Octahedral stress versus mean stress (left) and versus $(\sigma_1+\sigma_3)/2$ (right): true trial test on Santa Monica Beach sand (Dr=74%); data from (Wang and Lade, 2001)

Fig. 11 Predicted values of σ_a vs. σ_r compared to test results: compression (left); extension (right)

Figure 1

Click here to download high resolution image

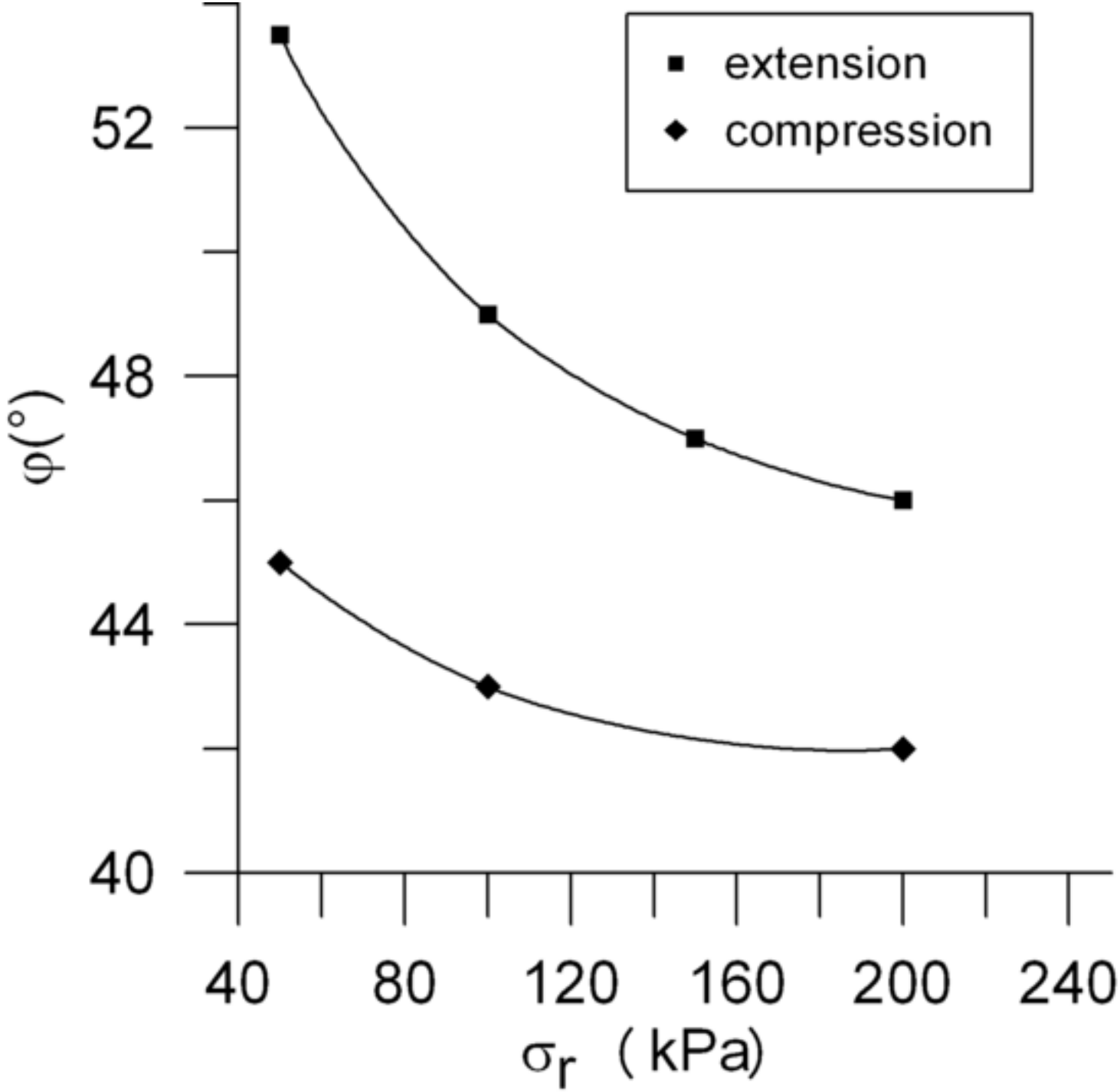

Figure 2

Click here to download high resolution image

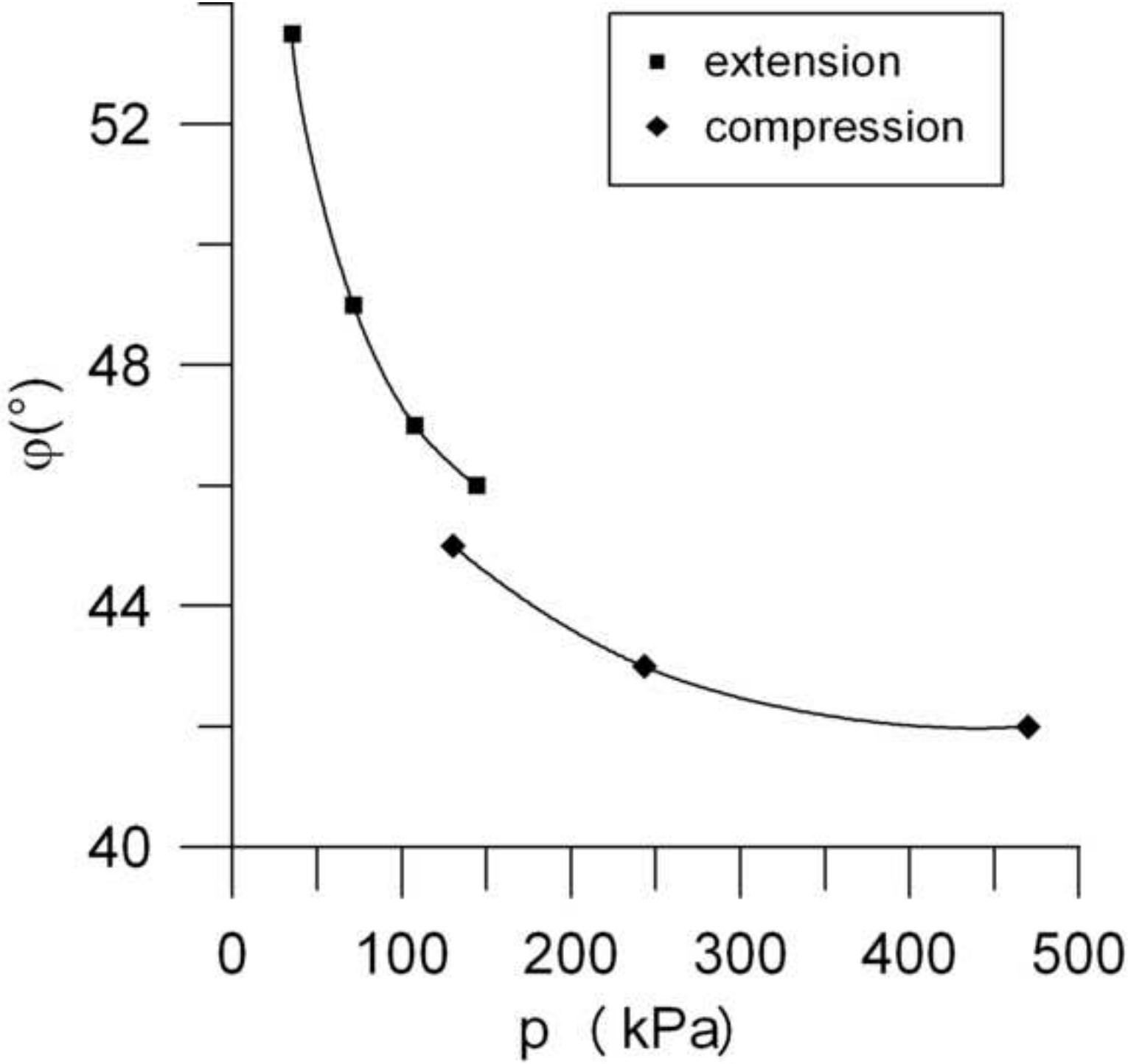

Figure 3

Click here to download high resolution image

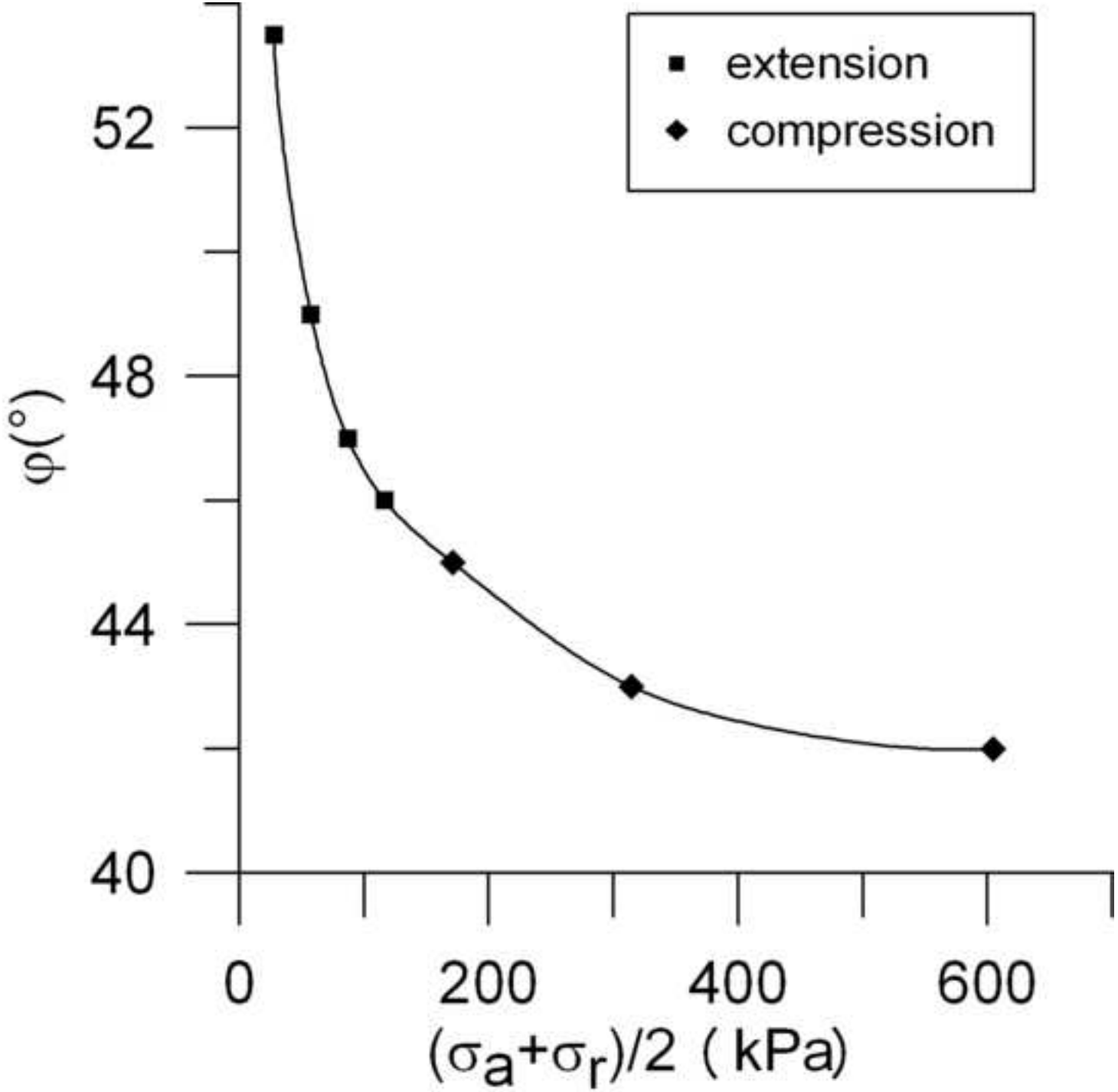

Figure 4

Click here to download high resolution image

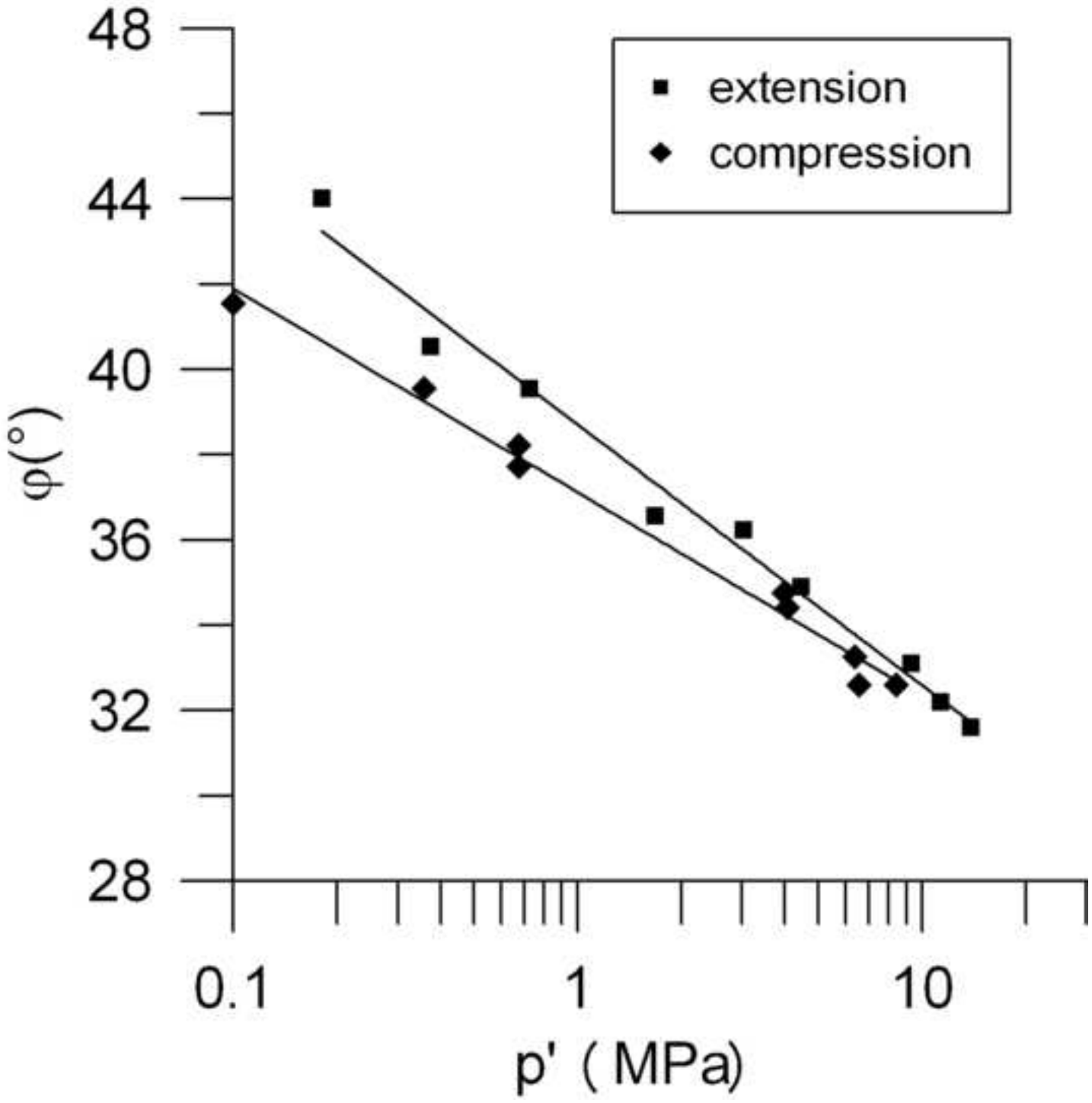

Figure 5

Click here to download high resolution image

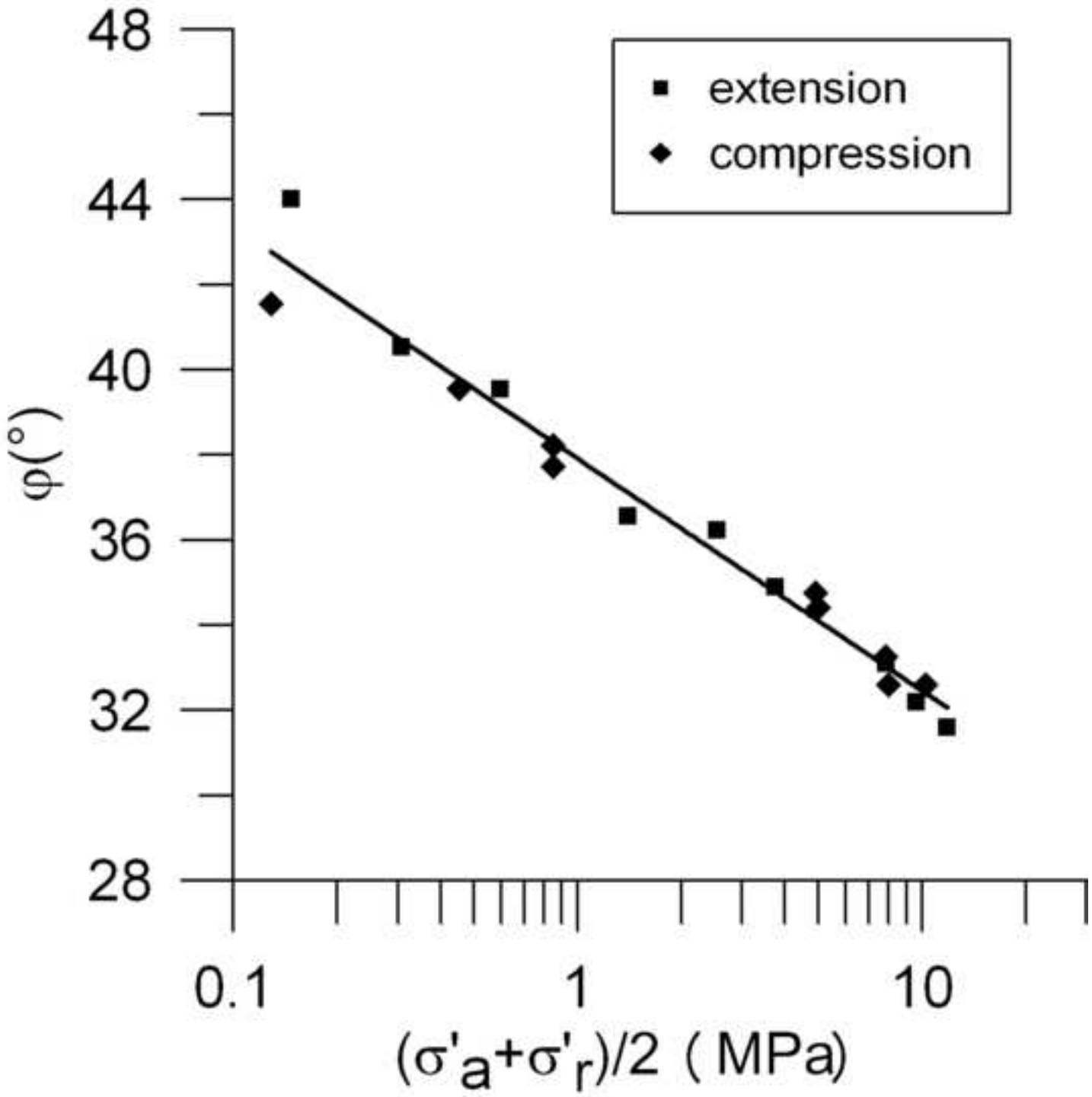

Figure 6

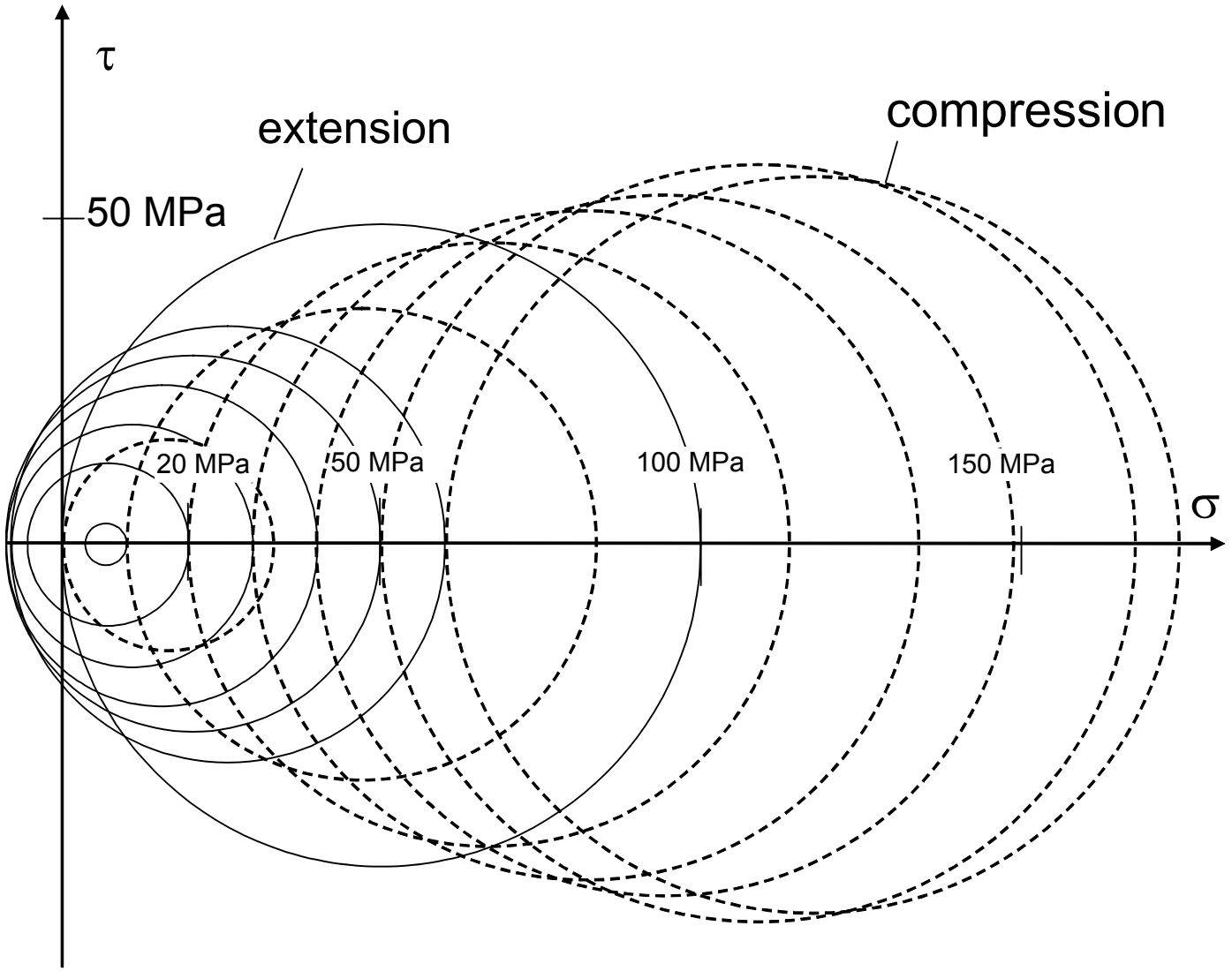

Figure 7

Click here to download high resolution image

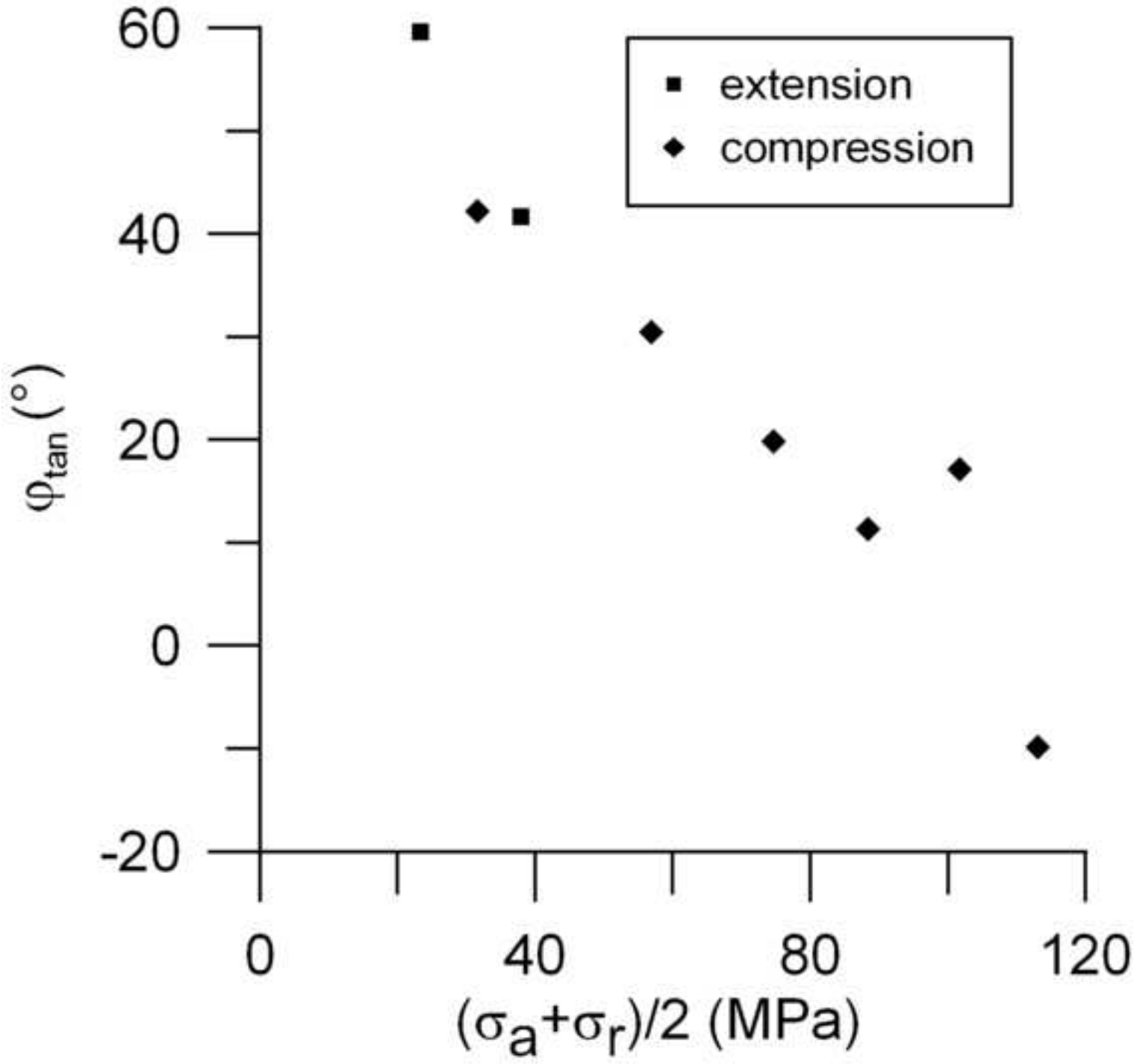

Figure 8

Click here to download high resolution image

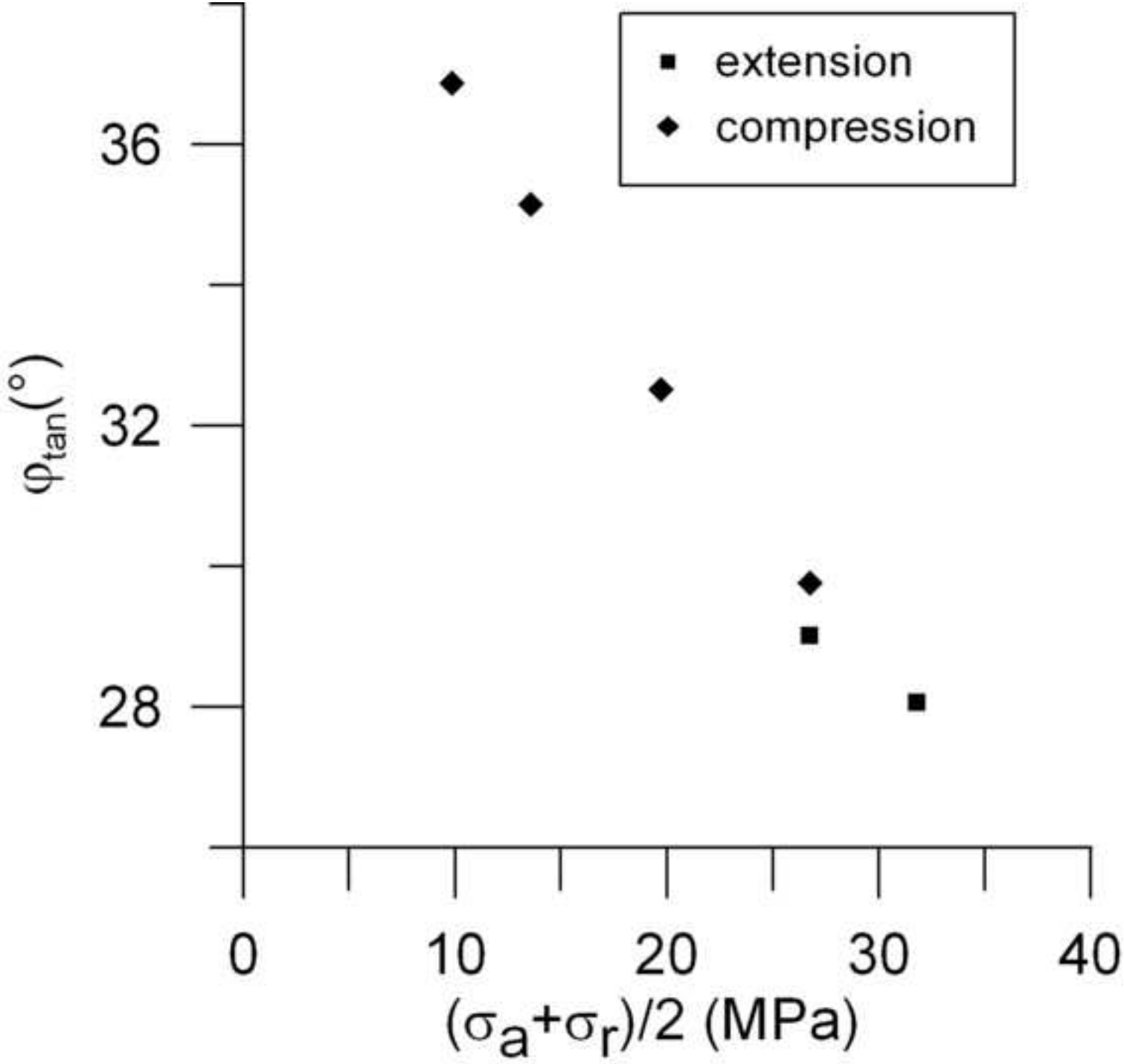

Figure 9
Click here to download high resolution image

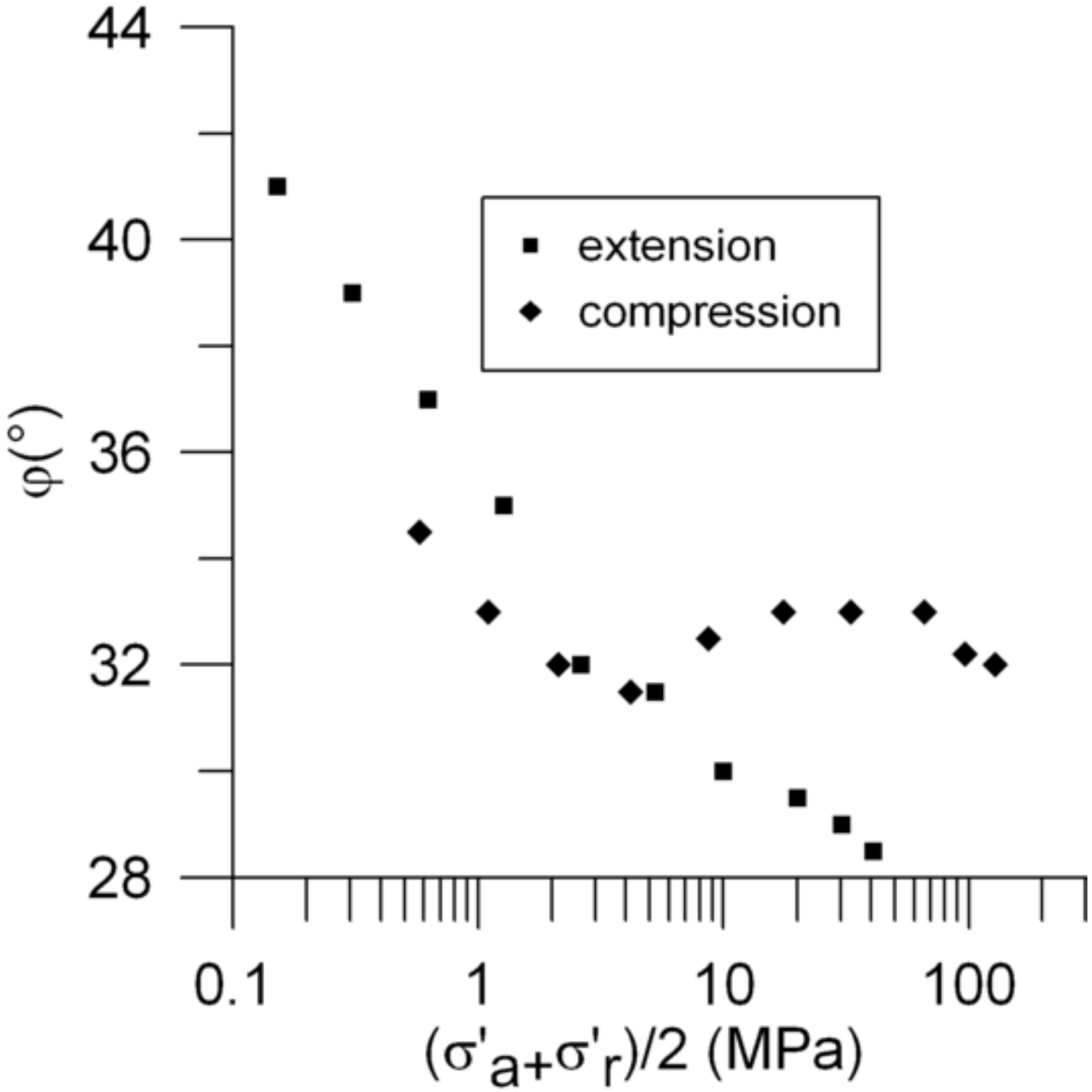

Figure 10

Click here to download high resolution image

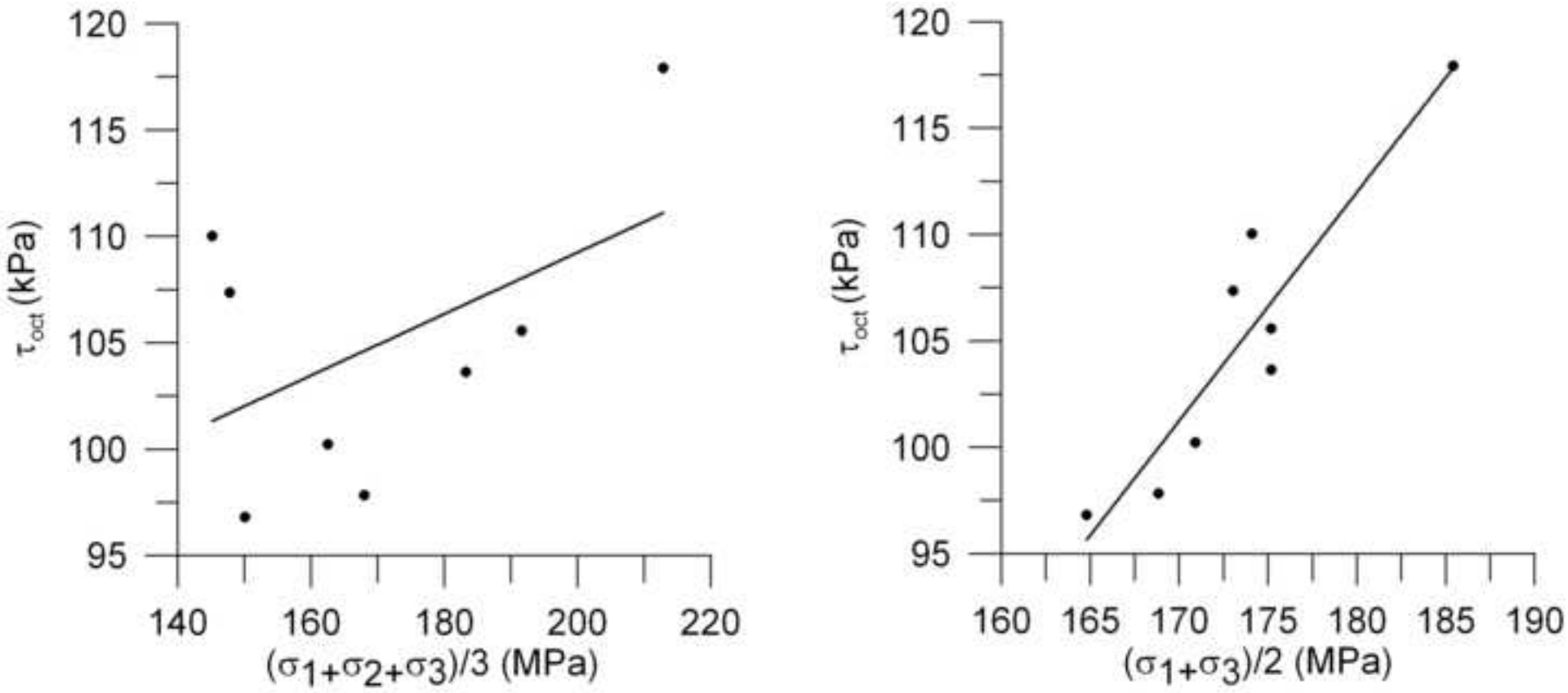

Figure 11

Click here to download high resolution image